

# Ground-State Fidelity and Kosterlitz-Thouless Phase Transition for Spin 1/2 Heisenberg Chain with Next-to-the-Nearest-Neighbor Interaction

Hong-Lei Wang, Ai-Min Chen, Bo Li and Huan-Qiang Zhou<sup>1</sup>

<sup>1</sup>Centre for Modern Physics and Department of Physics,  
Chongqing University, Chongqing 400044, The People's Republic of China

The Kosterlitz-Thouless transition for the spin 1/2 Heisenberg chain with the next-to-the-nearest-neighbor interaction is investigated in the context of an infinite matrix product state algorithm, which is a generalization of the infinite time-evolving block decimation algorithm [G. Vidal, Phys. Rev. Lett. **98**, 070201 (2007)] to accommodate both the next-to-the-nearest-neighbor interaction and spontaneous dimerization. It is found that, in the critical regime, the algorithm automatically leads to infinite degenerate ground-state wave functions, due to the finiteness of the truncation dimension. This results in *pseudo* symmetry spontaneous breakdown, as reflected in a bifurcation in the ground-state fidelity per lattice site. In addition, this allows to introduce a pseudo-order parameter to characterize the Kosterlitz-Thouless transition.

PACS numbers: 03.67.-a, 64.60.A-, 05.70.Fh

## I. INTRODUCTION

Quantum phase transitions (QPTs)<sup>1</sup> is one of the most intriguing research subjects in condensed matter physics. A QPT occurs at absolute zero due to quantum fluctuations in a variety of quantum many-body systems. In the conventional Landau-Ginzburg-Wilson paradigm, a phase transition accompanies spontaneous symmetry breaking (SSB)<sup>2,3</sup> that is characterized by a local order parameter. However, it now becomes clear that not all QPTs fall into this category<sup>4</sup>. In fact, topological phase transitions do not involve any SSB. This even dates back to the Kosterlitz-Thouless (KT) transition<sup>5</sup>, first discovered for two-dimensional classical XY model. Actually, the KT transition is ubiquitous in one-dimensional quantum systems. It describes the instability of the Luttinger liquid under a marginal perturbation. Normally, it is not an easy task to determine whether or not the KT transition occurs in a specific system, because there are pathological problems to analyze the KT transition numerically. One of these problems is that the finite size scaling technique<sup>6</sup>, which is successful for second order QPTs<sup>1,4</sup>, can not be applied to the KT transition<sup>7</sup>, since there are logarithmic corrections from the marginal perturbation.

Recently, a novel approach to QPTs in quantum many-body lattice systems has been put forward<sup>8-14</sup>, which is based on fidelity, a measure of quantum state distinguishability, in quantum information science. As argued in Refs.<sup>9,10</sup>, the ground-state fidelity per lattice site is able to capture quantum criticality underlying many-body physics in condensed matter. This fact, combining with a practical means to compute the ground-state fidelity per lattice site for infinite-size quantum lattice systems, make it practical to investigate critical phenomena in quantum many-body systems. Coincidentally, recent developments in the context of the tensor network (TN) algorithms for translation-invariant quantum lattice systems offer such a practical means. Here, we mention the infinite matrix product state (iMPS) algorithm<sup>15</sup> in one spatial dimension and the infinite projected entangled-pair states (iPEPS)<sup>16</sup> in two or higher spatial dimensions. These algorithms exploit the translation invariance of the system and parallelizability of

a TN representation of quantum many-body wave functions, which provides an efficient way to classically simulate quantum many-body lattice systems.

In a previous work<sup>17</sup>, we have succeeded in applying the fidelity per site approach to study the KT transition in both the one-dimensional spin 1/2 XXZ model and the spin 1 XXZ model with uniaxial single-ion anisotropy. This results in the introduction of a novel concept-*pseudo* SSB, offering a novel perspective to understand the KT transition, in the conventional Landau-Ginzburg-Wilson paradigm, from the iMPS representation. As such, it resolved the controversy regarding whether or not the ground-state fidelity is able to detect the KT QPTs<sup>13</sup>. However, more work is needed to clarify if such an approach is applicable to the KT transition in other quantum many-body lattice systems.

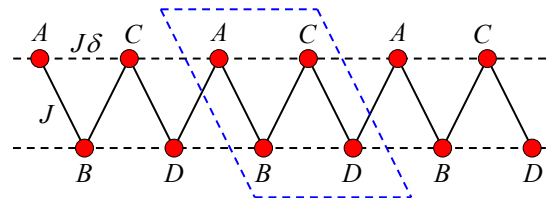


FIG. 1: (Color online) A sketch for the zigzag chain with the nearest-neighbor (NN) and next-to-the nearest-neighbor (NNN) interactions  $J$  and  $J\delta$ . The parameter  $\delta$  represents the ratio between the NNN coupling and the NN coupling. The dash-line box indicates the unit cell.

In this paper, we propose an iMPS algorithm, a generalization of the infinite time-evolving block decimation algorithm<sup>15</sup>, which allows us to accommodate both the next-to-the-nearest-neighbor interaction and spontaneous dimerization. It is found that, in the critical regime, the algorithm automatically leads to infinite degenerate ground-state wave functions, due to the finiteness of the truncation dimension. This results in *pseudo* symmetry spontaneous breakdown, as reflected in a bifurcation in the ground-state fidelity per lattice site. In addition, this allows to introduce a pseudo-order parameter to characterize the KT transition, which must be

scaled down to zero in order to be consistent with the Mermin-Wagner theorem<sup>18</sup>.

## II. MATRIX PRODUCT STATE ALGORITHM ON AN INFINITE-SIZE ONE-DIMENSIONAL LATTICE

Suppose the model Hamiltonian takes the form:  $H = \sum_i h^{[i, i+1, i+2]}$ , with  $h^{[i, i+1, i+2]}$  being the sum of the nearest-neighbor and the next-to-the-nearest-neighbor three-body Hamiltonian density. A realization of such a model Hamiltonian in the zigzag chain is shown in Fig. 1. To take account of a possible dimerization arising from the competition between quantum fluctuations and geometric frustration, we choose four sequential sites ( $A, B, C, D$ ) as a unit cell. Starting with a randomly chosen initial state  $|\Psi(0)\rangle$ , which is not orthogonal to the genuine ground state, a ground-state wave function can be computed by the imaginary time evolution  $|\Psi_g\rangle = \exp(-H\tau)|\Psi(0)\rangle / \|\exp(-H\tau)|\Psi(0)\rangle\|$  with  $\tau \rightarrow \infty$ . To realize the imaginary time evolution operation, the imaginary time  $\tau$  is divided into many small slices  $\delta\tau = \tau/N$  to approximate the continuous time evolution by a sequence of small gates. Meanwhile, the time evolution operator is expanded to a product of evolution operators acting on three sites:  $U_3 = \exp(-h^{[i, i+1, i+2]}\delta\tau)$  with  $\delta\tau \ll 1$ , as follows from the Suzuki-Trotter decomposition<sup>19</sup>. Any wave function admits an iMPS representation in a canonical form: attached to each site a four-index tensor  $\Gamma_n^{sr}$  and each bond a diagonal matrix  $\lambda_n$ , where  $n = A, B, C$  and  $D$ . Here,  $s$  is a physical index,  $s = 1, \dots, d$ , with  $d$  being the dimension of the local Hilbert space.  $l$  and  $r$  denote the bond indices,  $l, r = 1, \dots, \chi$ , with  $\chi$  being the truncation dimension. For simplicity, we use  $\Gamma_n$  instead of  $\Gamma_n^{sr}$  in the text below.

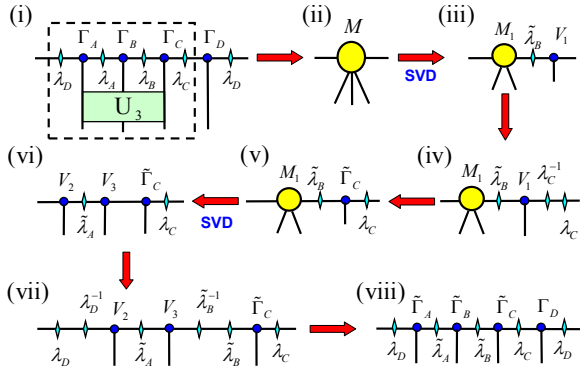


FIG. 2: (Color online) The updating procedure for the tensors  $\Gamma_n$  and the diagonal matrices  $\lambda_n$  ( $n = A, B, C$  and  $D$ ): (i) Apply the three-site gate  $U_3$ . one needs to update the tensors  $\Gamma_A, \Gamma_B, \Gamma_C$ , and the diagonal matrices  $\lambda_A, \lambda_B$ ; (ii) Contract the tensors inside the dash-line box in (i) into a single tensor  $M$ ; (iii) Reshape  $M$  into a matrix and perform a singular value decomposition (SVD); (iv) Insert the identity resolution on the right hand side; (v) Update the tensor  $\tilde{\Gamma}_C$ ; (vi) Perform an SVD for the matrix contracted from  $M_1$  and  $\tilde{\lambda}_B$ ; (vii) Insert the identity resolution; (viii) All the tensors  $\tilde{\Gamma}_A, \tilde{\Gamma}_B, \tilde{\Gamma}_C$ , and the diagonal matrices  $\tilde{\lambda}_A$  and  $\tilde{\lambda}_B$  are updated.

The updating procedure for the tensors  $\Gamma_n$  and the diagonal matrices  $\lambda_n$  ( $n = A, B, C$  and  $D$ ) in the iMPS representation under the action of the three-site gate  $U_3$  is visualized in Fig. 2: (i) Apply the three-site gate  $U_3$  onto the iMPS tensors  $\Gamma_A, \Gamma_B$  and  $\Gamma_C$ . The tensors involved in this action is shown in the dash-line box. (ii) Contract the tensors  $\lambda_D, \Gamma_A, \lambda_A, \Gamma_B, \lambda_B, \Gamma_C$  and  $\lambda_C$  into a single tensor and reshape the tensor into a  $\chi d^2 \times \chi d$  matrix  $M$ . (iii) Perform a singular value decomposition (SVD) to the matrix  $M$ . After truncating and reshaping, we get the tensors  $M_1, V_1$  and the updated diagonal matrix  $\tilde{\lambda}_B$ . (iv) Insert the identity resolution  $I = \lambda_C^{-1} \lambda_C$  on the right hand side and contract the tensors  $V_1$  and  $\lambda_C^{-1}$  to get the updated  $\tilde{\Gamma}_C$ , as done in step (v). (vi) Contract  $M_1$  and  $\tilde{\lambda}_B$  into a matrix and perform a SVD again, one gets the tensors  $V_2, V_3$  and the updated  $\tilde{\lambda}_A$ . (vii) Insert the identity resolution; (viii) All the tensors  $\tilde{\Gamma}_A, \tilde{\Gamma}_B, \tilde{\Gamma}_C$ , and the diagonal matrices  $\tilde{\lambda}_A$  and  $\tilde{\lambda}_B$  are updated. Shifting the action of the three-site gate  $U_3$  one site each time and repeating four times, we are able to update the tensors under the imaginary time evolution of an slice  $\delta\tau$ . Repeat the procedure until the ground-state energy per lattice converges, an approximate ground-state wave function is generated in the iMPS representation.

## III. MODEL

Consider a spin 1/2 Heisenberg chain with the nearest-neighbor coupling  $J$  and next-to-the-nearest-neighbor coupling  $J\delta$ . It is described by the Hamiltonian

$$H = J \sum_{i=-\infty}^{\infty} (\mathbf{S}^{[i]} \cdot \mathbf{S}^{[i+1]} + \delta \mathbf{S}^{[i]} \cdot \mathbf{S}^{[i+2]}), \quad (1)$$

where  $\mathbf{S}^{[i]}$  are the spin-1/2 Pauli operators at the  $i$ -th site. The system is equivalent to a zigzag chain as shown in Fig. 1. We set the nearest-neighbor antiferromagnetic coupling  $J = 1$  as the energy scale and consider the ratio interval  $0 \leq \delta \leq 0.5$ . The system undergoes the KT transition at  $\delta_c \sim 0.2411$ <sup>20</sup>: the Luttinger liquid state for  $\delta < \delta_c$  and the dimerized state for  $\delta > \delta_c$ <sup>21</sup>, respectively. Actually, the KT transition accompanies a discrete  $Z_2$  SSB in the dimerized phase.

## IV. GROUND-STATE FIDELITY PER LATTICE SITE

The ground-state fidelity per lattice site,  $d(\delta_1, \delta_2)$ , with  $\delta$  being the control parameter, is defined as the scaling parameter:  $F(\delta_1, \delta_2) \sim d(\delta_1, \delta_2)^N$ , with  $N$  the total number of the lattice sites, and  $F(\delta_1, \delta_2) \equiv |\langle \Psi(\delta_2) | \Psi(\delta_1) \rangle|$  between two ground-state wave functions  $|\Psi(\delta_1)\rangle$  and  $|\Psi(\delta_2)\rangle$ . It characterizes how fast the fidelity  $F(\delta_1, \delta_2)$  varies when the thermodynamic limit is approached<sup>9,10</sup>. In fact, the ground-state fidelity per lattice site  $d(\delta_1, \delta_2)$  may be regarded as a partition function per site of a classical statistical vertex lattice model defined on the same lattice. That explains why  $d(\delta_1, \delta_2)$  is able to detect QPTs<sup>22</sup>. That is, the ground-state fidelity per lattice site exhibits a singular behavior when the control parameter  $\delta$  crosses a transition point  $\delta_c$ .

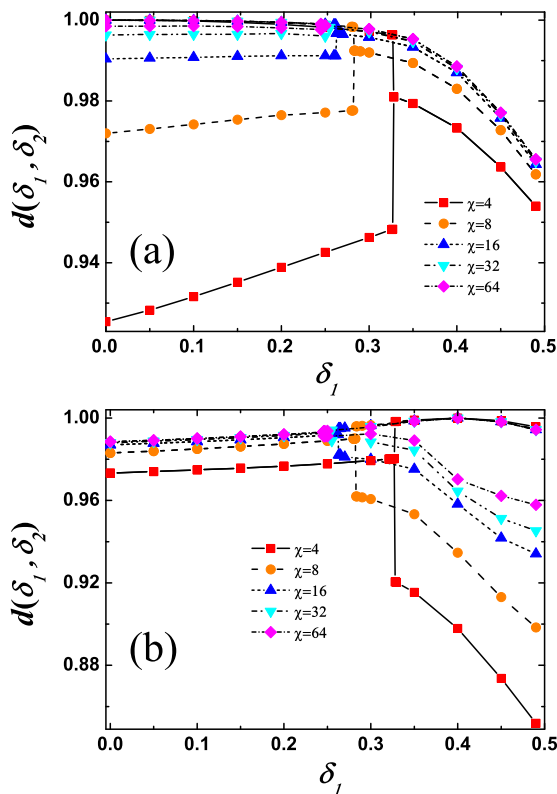


FIG. 3: (Color online) The ground-state fidelity per lattice site,  $d(\delta_1, \delta_2)$ , for the spin 1/2 Heisenberg chain with the NNN interaction. We have chosen  $\Psi(\delta_2)$  as a reference state, with  $\delta_2$  in different phases: (a)  $\delta_2 = 0$  in the  $SU(2)$  symmetry-broken phase. There is a bifurcation point in  $d(\delta_1, \delta_2)$ , which tends to disappear, when  $\chi$  approaches  $\infty$ . (b)  $\delta_2 = 0.4$  in the  $Z_2$  symmetric-broken phase. A bifurcation point always exists whatever the truncation dimension  $\chi$  we choose, as it should be for a discrete symmetry SSB. Therefore, the ground-state fidelity per lattice site,  $d(\delta_1, \delta_2)$ , is able to distinguish degenerate ground states, with a (pseudo) critical point as a bifurcation point.

Fig. 3 shows the ground-state fidelity per lattice site,  $d(\delta_1, \delta_2)$ , as a function of  $\delta_1$ , when  $\delta_2$  is fixed, for the Heisenberg model with the NNN interaction, for different values of the truncation dimension  $\chi$ . The iMPS simulation is performed for a randomly chosen initial state. It automatically induces degenerate ground-state wave functions, which break the  $SU(2)$  symmetry in the Luttinger liquid phase and the  $Z_2$  symmetry in the dimer phase.

In Fig. 3(a), the reference state  $\Psi(\delta_2 = 0)$  is chosen in the  $SU(2)$  symmetry-broken phase. The ground-state fidelity per lattice site,  $d(\delta_1, \delta_2)$ , takes infinitely many values lying between two extreme values, as a consequence of degenerate ground states, whereas in the  $Z_2$  symmetry-broken phase,  $d(\delta_1, \delta_2)$  yields just one value. A bifurcation point occurs, which coincides with the pseudo-transition point  $\delta_c^\chi$ . With increasing  $\chi$ , the difference between two extreme values of  $d(\delta_1, \delta_2)$  decreases. Note that, the bifurcation point tends to disappear when  $\chi$  goes to infinity, implying that degener-

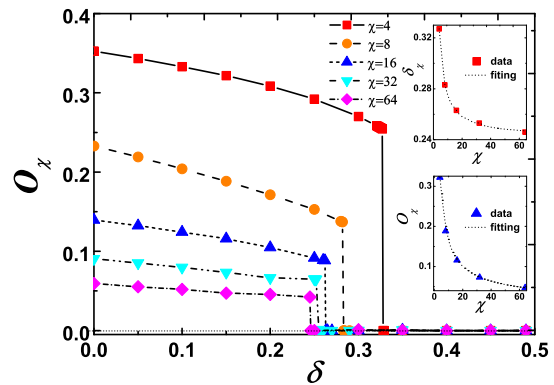


FIG. 4: (Color online) The pseudo-local-order parameter  $O_\chi$  as a function of  $\delta$ . The iMPS simulation is performed for a randomly chosen initial state. An extrapolation of the pseudo critical point  $\delta_c^\chi$  is performed for pseudo-transition points, at which the pseudo-order parameter become zero, yielding the KT transition point  $\delta_c = 0.2418$  in the right-top inset. The right-down inset shows that, in the critical phase, the pseudo-order parameter is scaled down to zero according to  $O_\chi = a\chi^{-b}(1 + c\chi^{-1})$ , with  $a=0.5993$ ,  $b=0.6150$ ,  $c=1.0379$ , to keep consistent with the Mermin-Wagner theorem.

ate ground states arise from the finiteness of the truncation dimension, an artifact of the iMPS algorithm. In fact, all the degenerate ground states should collapse into the genuine ground state as  $\chi$  approaches  $\infty$ , as required to keep consistent with the Mermin-Wagner theorem: no continuous symmetry is spontaneously broken in one-dimensional quantum systems. However, the critical point  $\delta_c$  may be determined by performing an extrapolation with respect to a few reasonably small  $\chi$ 's.

In Fig. 3(b), the reference state  $\Psi(\delta_2 = 0.4)$  is chosen in the  $Z_2$  symmetry-broken phase. Bifurcation points occur again in the ground-state fidelity per lattice site. However, they never vanish, when  $\chi$  approaches  $\infty$ . Instead, they tend to saturate when  $\chi$  increases. This is expected, since bifurcation points arise from the discrete group  $Z_2$  SSB.

Therefore, we conclude that, for a finite truncation dimension  $\chi$ , the ground-state fidelity per lattice site,  $d(\delta_1, \delta_2)$ , is able to distinguish degenerate ground-state wave functions with a reference state in the symmetry-broken phase. In addition, the iMPS algorithm enables us to locate the KT transition point accurately by computing the ground-state fidelity per lattice site,  $d(\delta_1, \delta_2)$ , with a moderate computational cost.

## V. PSEUDO ORDER PARAMETER

As is well known, the iMPS algorithm yields the best approximation to a ground-state wave function for a gapful lattice system. However, for a gapless system with continuous symmetry, if the truncation dimension  $\chi$  is finite, the iMPS algorithm automatically produces infinitely many degenerate ground states from a randomly chosen initial state<sup>17</sup>, each of which breaks the continuous symmetry. That is, a numeri-

cal phenomenon occurs, which shares all the features of an SSB resulting from random perturbations. Such a pseudo-symmetry-broken order may be quantified by introducing a pseudo-local-order parameter, which may be read off from a reduced density matrix on a local area<sup>22</sup>. However, this phenomenon is in contradiction with the Mermin-Wagner theorem, which states that no continuous symmetry is spontaneously broken for quantum systems in one spatial dimension<sup>18</sup>. To resolve this apparent contradiction, one has to require that the pseudo-local-order parameter must be scaled down to zero, when the truncation dimension  $\chi$  goes to  $\infty$ . We emphasize that both *pseudo* SSB and *pseudo*-local-order parameter arise from the artifact of the iMPS algorithm, in sharp contrast with a genuine SSB and a local order parameter.

In the Heisenberg model with the NNN interaction, the pseudo-local-order parameter may be chosen as  $O_\chi = \sqrt{\langle S_x^i \rangle^2 + \langle S_y^i \rangle^2 + \langle S_z^i \rangle^2}$  for the truncation dimension  $\chi$ . The pseudo-local-order parameter  $O_\chi$  is plotted as a function of  $\delta$  in Fig. 4. The iMPS simulation is performed for a randomly chosen initial state, with the truncation dimension  $\chi$  to be 4, 8, 16, 32, and 64, respectively. Notice that  $\hat{O}_\chi$  is zero in the  $Z_2$  symmetry-broken phase, but nonzero in the pseudo  $SU(2)$  symmetry-broken phase, due to the finiteness of the truncation dimension  $\chi$ . However, this is nothing but an artifact of the iMPS algorithm. Remarkably, one may take advantage of this artifact to locate a critical point  $\delta_c^\chi$ . Note that an extrapolation with respect to  $\chi$  may be performed for the pseudo-phase-transition points  $\delta_c^\chi$ , at which the pseudo-local-order parameter becomes zero. In the right-top inset of Fig. 4, the KT transition point  $\delta_c = 0.2418$  is determined from such an extrapolation, which is comparable with  $\delta_c = 0.2411$  from

the level spectroscopy analysis<sup>20</sup>. Here, we require that the pseudo-local-order parameter must vanish, when  $\chi$  goes to  $\infty$ , to keep consistent with the Mermin-Wagner theorem. Therefore, a fitting function  $O_\chi = a\chi^{-b}(1 + c\chi^{-1})$  is chosen, with  $a=0.5993$ ,  $b=0.6150$ ,  $c=1.0379$ , as shown in the right-down inset in Fig. 4. This ensures that, when  $\chi \rightarrow \infty$ , all the degenerate ground states collapse into the genuine ground state.

## VI. CONCLUSION

We have investigated the KT transition for the spin 1/2 Heisenberg chain with the NNN interaction in the context of an iMPS algorithm, a generalization of the infinite time-evolving block decimation algorithm to accommodate both the next-nearest-neighbor interaction and spontaneous dimerization. It is demonstrated that, in the critical regime, the algorithm automatically leads to infinitely many degenerate ground-state wave functions, due to the finiteness of the truncation dimension. This results in *pseudo* symmetry spontaneous breakdown, as reflected in a bifurcation in the ground-state fidelity per lattice site. In addition, this allows to introduce a pseudo-local-order parameter to characterize the KT transition, which scales down to zero when  $\chi$  approaches infinity.

## Acknowledgements

The work is supported by the National Natural Science Foundation of China (Grant No: 10874252) and the Fundamental Research Funds for Central Universities (Project No. CDJXS11102213).

- 
- <sup>1</sup> S. Sachdev, *Quantum Phase Transition* (Cambridge University Press, Cambridge, 1999).
- <sup>2</sup> P. W. Anderson, *Basic Notions of Condensed Matter Physics, Addison-Wesley: The Advanced Book Program* (Addison-Wesley, Reading, MA, 1997).
- <sup>3</sup> S. Coleman, *An Introduction to Spontaneous Symmetry Breakdown and Gauge Fields: Laws of Hadronic Matter*, ed. A. Zichichi (Academic, New York, 1975).
- <sup>4</sup> X.-G. Wen, *Quantum Field Theory of Many-Body Systems* (Oxford University Press, Oxford, 2004).
- <sup>5</sup> J. M. Kosterlitz and D. J. Thouless, *J. Phys. C* **6**, 1181 (1973); J. M. Kosterlitz, *J. Phys. C* **7**, 1046 (1974).
- <sup>6</sup> M. N. Barber, *Phase Transitions and Critical Phenomena*, ed. C. Domb and J. L. Lebowitz (Academic, London, 1983), Vol. 8.
- <sup>7</sup> J. Sólyom and T. A. L. Ziman, *Phys. Rev. B* **30**, 3980 (1984); R. G. Edwards, J. Goodman, and A. D. Sokal, *Nucl. Phys. B* **354**, 289 (1991).
- <sup>8</sup> P. Zanardi and N. Paunković, *Phys. Rev. E* **74**, 031123 (2006).
- <sup>9</sup> H.-Q. Zhou and J. P. Barjaktarević, *J. Phys. A: Math. Theor.* **41**, 412001 (2008); H.-Q. Zhou, J.-H. Zhao, and B. Li, *J. Phys. A: Math. Theor.* **41**, 492002 (2008); H.-Q. Zhou, arXiv: 0704.2945.
- <sup>10</sup> H.-Q. Zhou, R. Orús, and G. Vidal, *Phys. Rev. Lett.* **100**, 080601 (2008).
- <sup>11</sup> P. Zanardi, M. Cozzini, and P. Giorda, *J. Stat. Mech.* L02002, (2007); N. Oelkers and J. Links, *Phys. Rev. B* **75**, 115119 (2007); M. Cozzini, R. Ionicioiu, and P. Zanardi, *Phys. Rev. B* **76**, 104420 (2007); L. Campos Venuti and P. Zanardi, *Phys. Rev. Lett.* **99**, 095701 (2007).
- <sup>12</sup> W.-L. You, Y.-W. Li, and S.-J. Gu, *Phys. Rev. E* **76**, 022101 (2007); S. J. Gu, H. M. Kwok, W. Q. Ning, and H. Q. Lin, *Phys. Rev. B* **77**, 245109 (2008); M. F. Yang, *Phys. Rev. B* **76**, 180403(R) (2007); Y. C. Tzeng and M. F. Yang, *Phys. Rev. A* **77**, 012311 (2008); J. O. Fjærestad, *J. Stat. Mech.: Theory Exp.* (2008) P07011; T. Liu, Y.-Y. Zhang, Q.-H. Chen, and K.-L. Wang, *Phys. Rev. A* **80**, 023810 (2009); J. Sirker, *Phys. Rev. Lett.* **105**, 117203 (2010).
- <sup>13</sup> S. Chen, L. Wang, Y. Hao, and Y. Wang, *Phys. Rev. A* **77**, 032111 (2008); S. Chen, L. Wang, S.-J. Gu, and Y. Wang, *Phys. Rev. E* **76**, 061108 (2007).
- <sup>14</sup> M. M. Rams and B. Damski, *Phys. Rev. Lett.* **106**, 055701 (2011).
- <sup>15</sup> G. Vidal, *Phys. Rev. Lett.* **98**, 070201 (2007).
- <sup>16</sup> F. Verstraete, and J. I. Cirac, e-print arXiv:cond-mat/0407066.
- <sup>17</sup> H.-L. Wang, J.-H. Zhao, B. Li, and H.-Q. Zhou, arXiv: 0902.1670.
- <sup>18</sup> N. D. Mermin and H. Wagner, *Phys. Rev. Lett.* **17**, 1133 (1966).
- <sup>19</sup> M. Suzuki, *Phys. Lett. A* **146**, 319 (1990).
- <sup>20</sup> K. Okamoto and K. Nomura, *Phys. Lett. A* **169**, 433 (1992).
- <sup>21</sup> F. D. M. Haldane, *Phys. Rev. B* **25**, 4925 (1982).
- <sup>22</sup> H.-Q. Zhou, arXiv: 0803.0585.